NASA Technical Memorandum 4314

Target Correlation Effects on Neutron-Nucleus Total, Absorption, and Abrasion Cross Sections

Francis A. Cucinotta, Lawrence W. Townsend, and John W. Wilson

DECEMBER 1991

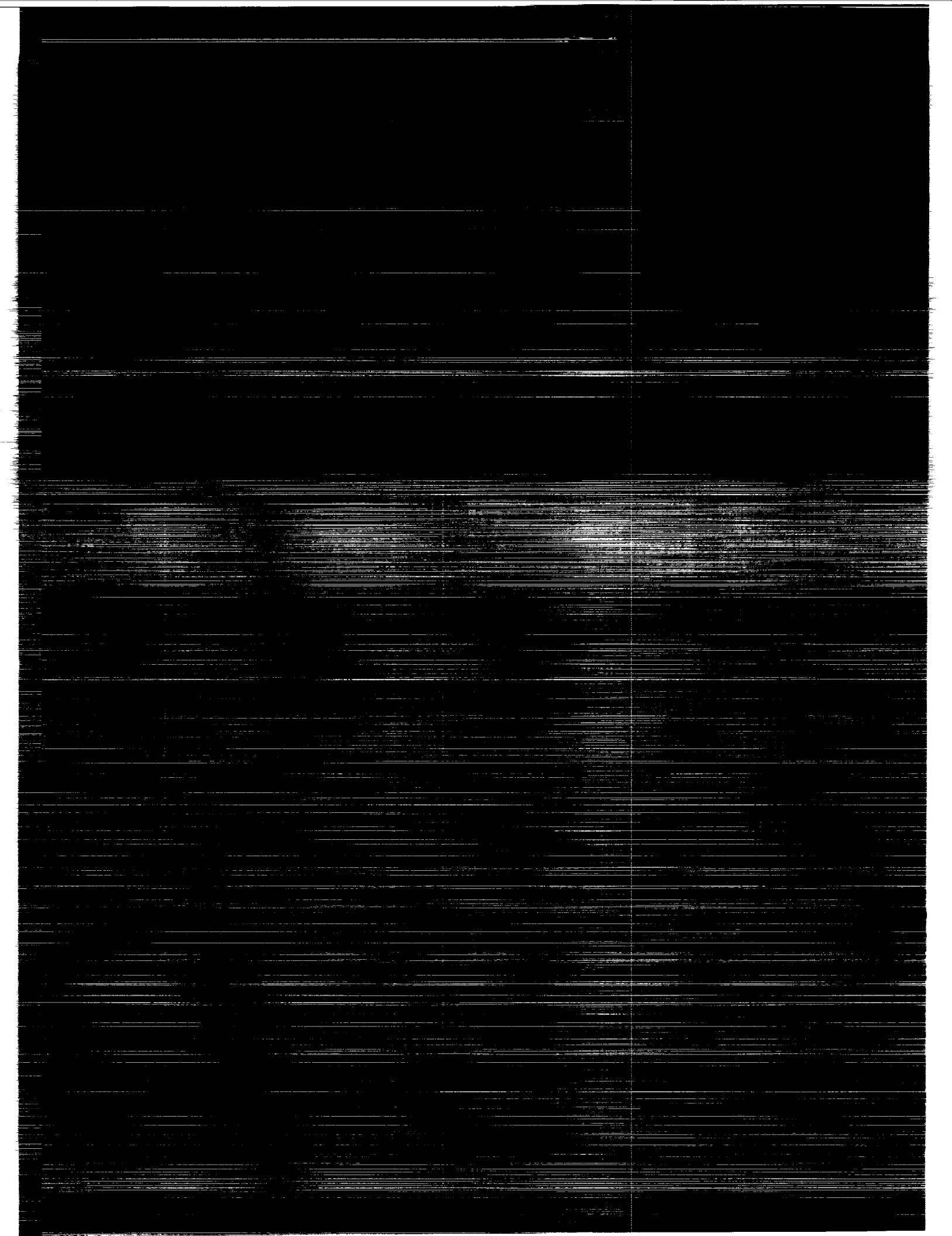

NASA Technical Memorandum 4314

Target Correlation Effects on Neutron-Nucleus Total, Absorption, and Abrasion Cross Sections

Francis A. Cucinotta, Lawrence W. Townsend, and John W. Wilson
Langley Research Center
Hampton, Virginia

National Aeronautics and Space Administration
Office of Management
Scientific and Technical Information Program
1991

Abstract

Second-order optical model solutions to the elastic scattering amplitude were used to evaluate total, absorption, and abrasion cross sections for neutron-nucleus scattering. Improved agreement with experimental data for total and absorption cross sections is found when compared with first-order (coherent approximation) solutions, especially below several hundred MeV. At higher energies, the first- and second-order solutions are similar. There are also large differences in abrasion cross-section calculations; these differences indicate a crucial role for cluster knockout in the abrasion step.

I. Introduction

The assessment of radiation risk to humans, in both their natural and space environments, from cosmic radiation is currently an area of active investigation. Predictions of biological damage will ultimately require a knowledge of the particle fluence spectra at the endpoint of interest. In turn, these particle fluence spectra are determined from charged-particle transport codes, which must contain a description of all important physical processes that occur as the incident ions and subsequent-generation fragment nuclei pass through natural and protective radiation shielding.

Recent studies (refs. 1 and 2) have shown the importance of using accurate energy-dependent, nuclear-interaction cross sections for the determination of fluence spectra for high-energy nuclei. A theoretical model for the prediction of cross sections is extremely useful, as it cannot be expected that enough experiments will be performed for all the collision pairs and energies of interest in cosmic-ray studies. In previous studies (refs. 3 to 6), a nuclear-interaction theory based on an effective coupled-channel solution to the nuclear scattering problem was considered for the prediction of interaction cross sections. A first-order approximation to the elastic amplitude was applied within the eikonal approximation for the prediction of total, absorption, and abrasion cross sections and showed good agreement with available experimental data.

More recently, a second-order solution to the eikonal coupled-channels (ECC) model (refs. 7 to 9) was developed and was found to give improved accuracy over the first-order solutions in limited studies for several collision pairs and energies. In this report, neutron-nucleus total, absorption, and abrasion cross sections are considered by using the second-order ECC model in an effort to improve the prediction of nuclear-interaction cross sections at cosmic-ray energies.

In the first-order (coherent approximation) ECC model, all nuclear excitations are neglected in the evaluation of the elastic amplitude. The second-order solution is found in terms of the bordered interaction matrix, which includes all scatterings from the ground to excited states and subsequent decay to the ground state. However, cascades between excited states are neglected. The second-order solution can be expressed in terms of the two-particle form factors of the nuclear ground-state, which must include the effects of short-range correlations to accurately represent the large momentum-transfer region of the scattering. In this work, we use a simple model for the two-particle form factors based on the nuclear matter approximation. Following the procedure in reference 10, the combined effects of Pauli correlations and short-range dynamic correlations are taken into account through the use of an effective correlation length. To simplify the calculations, the zero-range approximation is used to evaluate the correlation terms. The effects of correlations between the projectile and target, to first order, are included following the method developed in reference 6.

The abrasion cross-section model is based on a geometric probability interpretation of the absorption cross section. The effects of target correlations on the abrasion cross section are also considered herein by redefining the geometric probability for nucleon removal in a manner consistent with the second-order ECC solution. Large differences are found in this manner between the first- and second-order solutions at the lowest energies considered in this report.

Section III contains details of the formalism of the second-order solution for the elastic amplitude and introduces the second-order model for the abrasion cross section. The physical inputs used in our calculations are also described. Comparisons are made in section IV between the first- and second-order solutions, and comparisons are made with experimental

data for calculations of absorption and abrasion cross sections.

II. Symbols

A_f	fragment mass number
A_P	mass number of projectile nucleus
A_T	mass number of target nucleus
B	slope parameter
$\mathbf{b}$	impact parameter
$C(\mathbf{q})$	correlation function
$F^{(i)}$	projectile i-particle form factor
f	nucleus-nucleus scattering amplitude
f_{NN}	nucleon-nucleon scattering amplitude
$G^{(i)}$	target i-particle form factor
k	relative wave number
k_{NN}	two-body relative wave number
l_c	correlation length, 0.86 fm
m	number of abraded nucleons
$P(\mathbf{b})$	probability of not removing a nucleon
$\mathbf{q}$	momentum transfer vector
r	internal nuclear coordinate
T	kinetic energy of neutron, MeV
α	ratio of real part to imaginary part of forward two-body amplitude
Γ	second-order eikonal phase
ρ_{CH}	target charge density
ρ_o	normalization of density
σ	cross section
χ	first-order eikonal phase
Ω	solid-angle phase

Subscripts and superscripts:

abs	absorption
c	correlation
dir	direct
ex	exchange
el	elastic
m	abrasion
NN	nucleon-nucleon
P	projectile
T	target
tot	total

III. Elastic Channel

In the bordered interaction solution to the optical-model coupled-channel equations, the elastic amplitude is found (refs. 7 to 9) as

$$f(\mathbf{q}) = \frac{-ik}{2\pi}\int d^2b \exp(-i\mathbf{q}\cdot\mathbf{b})\{\exp[i\chi(\mathbf{b})]\cos\Gamma(\mathbf{b}) - 1\} \tag{1}$$

where k is the relative wave number in the overall center-of-mass frame, $\mathbf{q}$ is the momentum transfer, and $\mathbf{b}$ is the impact parameter. In equation (1), χ is the first-order eikonal phase, which represents the elastic matrix element, and Γ is the correlation phase, which represents the summation over all double scatterings where states are excited from and then de-excited to the ground state. The first-order eikonal phase is written as

$$\chi(\mathbf{b}) = \chi_{\mathrm{dir}}(\mathbf{b}) - \chi_{ex}(\mathbf{b}) \tag{2}$$

where the exchange term takes into account correlation effects between projectile and target nucleons (ref. 6). These terms are written as

$$\chi_{\mathrm{dir}}(\mathbf{b}) = \frac{A_P A_T}{2\pi k_{NN}}\int d^2q \exp(i\mathbf{q}\cdot\mathbf{b})F^{(1)}(-\mathbf{q})G^{(1)}(\mathbf{q})f_{NN}(\mathbf{q}) \tag{3}$$

and

$$\chi_{ex}(\mathbf{b}) = \frac{A_P A_T}{2\pi k_{NN}}\int d^2q \exp(i\mathbf{q}\cdot\mathbf{b})F^{(1)}(-\mathbf{q})G^{(1)}(\mathbf{q}) \times \frac{1}{(2\pi)^2}\int d^2q' \exp(i\mathbf{q}'\cdot\mathbf{b})f_{NN}(\mathbf{q}+\mathbf{q}')C(\mathbf{q}') \tag{4}$$

where $F^{(1)}$ and $G^{(1)}$ are projectile and target ground-state one-body form factors, respectively, and f_{NN} is the two-body amplitude parameterized as

$$f_{NN}(\mathbf{q}) = \frac{\sigma(\alpha+i)}{4\pi}k_{NN}\exp\left(-\frac{1}{2}Bq^2\right) \tag{5}$$

where k_{NN} is the relative wave number in the two-body system, σ is the two-body cross section, B is the slope parameter, and α is the ratio of the real part to the imaginary part of the forward, two-body amplitude. Values for the energy-dependent σ, B,

and α are found in references 4 and 5. The correlation factor is found as

$$C(\mathbf{q}) = \frac{1}{4}\left(\frac{\pi}{d}\right)\exp\left(-q^2/4d^2\right) \tag{6}$$

in reference 6 with $d = 1.85$ fm^{-1}.

The one-body form factor is written in terms of the charge form factor as

$$F^{(1)}(\mathbf{q}) = F_{CH}(\mathbf{q})/F_p(\mathbf{q}) \tag{7}$$

where F_p is the proton form factor. For a harmonic well distribution,

$$F_{CH} = \left(1 - sq^2\right)\exp\left(-aq^2\right) \tag{8}$$

where values for parameters s and a are from reference 5. For nuclei where a Woods-Saxon density is appropriate ($A_T \geq 20$),

$$\rho_{CH}^{(r)} = \frac{\rho_o}{1 + \exp\left[(r - R)/c\right]} \tag{9}$$

An exact Fourier transform to obtain the charge form factor may be found in a series solution (ref. (11))

$$F_{CH}(\mathbf{q}) = \frac{4\pi}{q}\rho_o\phi(\mathbf{q}) \tag{10}$$

where

$$\phi(q) = \pi Rc\left\{\frac{-\cos(Rq)}{\sinh(\pi cq)} + \frac{\pi c}{R}\frac{\sin(Rq)\coth(\pi cq)}{\sinh(\pi cq)} - \frac{2c}{\pi R}\sum_{m=1}^{\infty}(-1)^m\frac{mcq\exp(-mR/c)}{\left[(cq)^2 + m^2\right]^2}\right\} \tag{11}$$

The series in equation (11) converges rapidly, and the first three or four terms are accurate for most applications. Values for the parameters c and R are taken from reference 5.

The second-order phase Γ was defined in references 7 to 9 and, for nucleon-nucleus scattering, reduces to

$$\Gamma^2(\mathbf{b}) = A_T\left(\frac{1}{2\pi k_{NN}}\right)^2\iint d^2q d^2q' \exp(i\mathbf{q}\cdot\mathbf{b})\exp(i\mathbf{q}\cdot\mathbf{b}') \times f_{NN}(\mathbf{q})f_{NN}(\mathbf{q}')\left[-A_T G^{(1)}(\mathbf{q})G^{(1)}(\mathbf{q}') + (A_T - 1)\,G^{(2)}(\mathbf{q},\mathbf{q}')\right] \tag{12}$$

where $G^{(2)}$ is the ground-state two-body form factor of the target. To simplify the evaluation of equation (12), the zero-range approximation (refs. 12 and 13) is used, where

$$\Gamma^2(\mathbf{b}) = -2\left[\frac{2\pi A_T f_{NN}(0)}{k_{NN}}\right]^2 l_c\int_{-\infty}^{\infty} dz\rho_{CH}^2(\mathbf{b},z) - \frac{1}{A_T}\chi_{\text{dir}}^2(\mathbf{b}) \tag{13}$$

and where the correlation length l_c is 0.86 fm, and z is the z-component of r.

The total cross section is found from the elastic amplitude by using the optical theorem as follows:

$$\sigma_{\text{tot}} = \frac{4\pi}{k}\text{Im}\ f(\mathbf{q} = 0) \tag{14}$$

Equations (1) and (14) show that

$$\sigma_{\text{tot}} = 4\pi\int_0^{\infty} b\,db\left\{1 - \frac{1}{2}\exp\left[-\text{Im}(\chi + \Gamma)\right]\cos\left[\text{Re}(\chi + \Gamma)\right] - \frac{1}{2}\exp\left[-\text{Im}(\chi - \Gamma)\right]\cos\left[\text{Re}(\chi - \Gamma)\right]\right\} \tag{15}$$

The total absorption cross section is found as follows:

$$\sigma_{\text{tot}} = \sigma_{\text{abs}} + \sigma_{el} \tag{16}$$

where σ_{el} is the total elastic cross section. Integrating equation (1) by using $d\Omega \approx d^2q/k^2$ and by using equations (15) and (16) yields

$$\sigma_{\text{abs}} = 2\pi\int_0^{\infty} b\,db\left\{1 - \frac{1}{2}\exp(-2\text{Im}\chi) \times \left[\cosh(2\text{Im}\Gamma) + \cos(2\text{Re}\Gamma)\right]\right\} \tag{17}$$

All the results of this section (i.e., eqs. (1), (15), and (17)) reduce to the coherent approximation in the limit $\Gamma \to 0$.

Another quantity of interest is the abrasion cross section, which gives the probability of knockout of any number of nucleons. As in references 4, 14, and 15, the absorption cross section is written as

$$\sigma_{\text{abs}} = 2\pi\int_0^{\infty} b\,db\left\{1 - [P(\mathbf{b})]^{A_T}\right\} \tag{18}$$

where $P(\mathbf{b})$ is the probability, as a function of impact parameter, of not removing a target nucleon. For the second-order solution, it follows from equations (17) and (18) that

$$[P(\mathbf{b})]^{A_T} = \frac{1}{2}\exp(-2\text{Im}\chi)\left[\cosh(2\text{Im}\Gamma) + \cos(2\text{Re}\Gamma)\right] \tag{19}$$

and the cross section for removal of m target nucleons is written as

$$\sigma_m = \binom{A_T}{m} 2\pi \int_0^\infty b\,db\,[1 - P(\mathbf{b})]^m\,[P(\mathbf{b})]^{A_T - m} \tag{20}$$

Because of the dependence of Γ^2 on $f_{NN}(0)$, equations (17) and (20) depend on values of α. The analogous coherent model solutions are independent of α.

Of special note is the question of whether the abrasion model as represented by equation (20) is valid when correlations among target nucleons are present. The abrasion model is essentially a "classical geometric" picture of nucleon knockout. The original model is closely related to an independent particle assumption (ref. 16), where cluster knockout is not considered. Correlation effects lead to such cluster knockouts. (See ref. 17.) Equation (20) does not address cluster effects and assumes only that nucleons are removed. Numerical calculations are considered next. Deviations between first- and second-order abrasion cross sections suggest regions where the abrasion model as represented by equation (20) is questionable.

IV. Results

Comparisons between calculations and experimental data are shown in figures 1 to 6 for the total and absorption cross section as a function of neutron energy. The solid line is the second-order model, the dashed line is the first-order model, and the experimental data (error bars) are from reference 18. Above a few hundred MeV, the calculations give similar results; below 300 MeV, the second-order solutions show better agreement with the data. The representation of Γ as given in equation (13) may not be valid below 100 MeV because of the closure assumption that is invoked (ref. 8).

The differences observed at low energies between first- and second-order solutions are large for abrasion cross-section calculations. (See figs. 7 to 9.) Differences of a factor of 2 or greater vary with the number of nucleons that are abraded. Results for abrasion cross sections at 100, 200, and 300 MeV are shown in tables 1 to 3. Clearly, redefining $P(\mathbf{b})$ to be consistent with the second-order optical model leads to a drastically different partitioning of abraded nucleons than with the previously studied coherent approximation.

V. Concluding Remarks

The second-order solution to eikonal coupled-channel equations leads to improved predictions of total and absorption cross sections for neutron-nucleus scattering. Using an abrasion probability function consistent with the second-order elastic amplitude leads to dramatically altered predictions of abrasion cross sections below 300 MeV neutron energy. The importance of future study of cluster knockouts in the abrasion step is clearly demonstrated. It would be interesting to extend the calculations presented herein to other projectiles. Calculations with ablation effects should be made and compared with experimental data for fragmentation cross sections.

NASA Langley Research Center
Hampton, VA 23665-5225
November 15, 1991

VI. References

1. Townsend, L. W.; and Wilson, J. W.: An Evaluation of Energy-Independent Heavy Ion Transport Coefficient Approximations. *Health Phys.*, vol. 54, no. 4, Apr. 1988, pp. 409–412.

2. Wilson, John W.; Chun, S. Y.; Buck, W. W.; and Townsend, L. W.: High Energy Nucleon Data Bases. *Health Phys.*, vol. 55, no. 5, Nov. 1988, pp. 817–819.

3. Wilson, John W.: Composite Particle Reaction Theory. Ph.D. Diss., College of William and Mary in Virginia, June 1975.

4. Townsend, Lawrence W.: *Optical-Model Abrasion Cross Sections for High-Energy Heavy Ions.* NASA TP-1893, 1981.

5. Townsend, Lawrence W.; and Wilson, John W.: *Tables of Nuclear Cross Sections for Galactic Cosmic Rays—Absorption Cross Sections.* NASA RP-1134, 1985.

6. Townsend, Lawrence W.: *Harmonic Well Matter Densities and Pauli Correlation Effects in Heavy-Ion Collisions.* NASA TP-2003, 1982.

7. Cucinotta, Francis A.; Khandelwal, Govind S.; Maung, Khin M.; Townsend, Lawrence W.; and Wilson, John W.: *Eikonal Solutions to Optical Model Coupled-Channel Equations.* NASA TP-2830, 1988.

8. Cucinotta, Francis A.: Theory of Alpha-Nucleus Collisions at High Energies. Ph.D. Thesis, Old Dominion Univ., 1988.

9. Cucinotta, F. A.; Khandelwal, G. S.; Townsend, L. W.; and Wilson, J. W.: Correlations in α-α Scattering and Semi-Classical Optical Models. *Phys. Lett.*, vol. B223, no. 2, June 8, 1989, pp. 127–132.

10. Moniz, E. J.; and Nixon, G. D.: High Energy Coherent Processes With Nuclear Targets. *Ann. Phys. (NY)*, vol. 67, no. 1, Sept. 1971, pp. 58–97.

11. Maung, Khin Maung; Deutchman, P. A.; and Royalty, W. D.: Integrals Involving the Three-Parameter Fermi

Function. *Canadian J. Phys.*, vol. 67, nos. 2 & 3, Feb.–Mar. 1989, pp. 95–99.

12. Glauber, R. J.; and Matthiae, G.: High-Energy Scattering of Protons by Nuclei. *Nucl. Phys.*, vol. B21, no. 1, Aug. 1, 1970, pp. 135–157.

13. Ahmad, I.: An Analysis of Some Proton-Nucleus Scattering Data at 1 GeV. *Nucl. Phys.*, vol. A247, no. 3, Aug. 11, 1975, pp. 418–440.

14. Hüfner, J.; Schäfer, K.; and Schürmann, B.: Abrasion-Ablation in Reactions Between Relativistic Heavy Ions. *Phys. Review*, vol. 12, ser. C, no. 6, Dec. 1975, pp. 1888–1898.

15. Bleszynski, M.; and Sander, C.: Geometrical Aspects of High-Energy Peripheral Nucleus-Nucleus Collisons. *Nucl. Phys. A*, vol. 326, nos. 2–3, Sept. 10, 1979, pp. 525–535.

16. Koltun, Daniel S.; and Schneider, David M.: Reactive Content of the First-Order Optical Potential. *Phys. Review Lett.*, vol. 42, no. 4, Jan. 22, 1979, pp. 211–214.

17. Cucinotta, Francis A.; Townsend, Lawrence W.; Wilson, John W.; and Khandelwal, Govind S.: *Inclusive Inelastic Scattering of Heavy Ions and Nuclear Correlations.* NASA TP-3026, 1990.

18. Barashenkov, V. S.; Gudima, K. K.; and Toneev, V. D.: Cross Sections for Fast Particles and Atomic Nuclei. *Prog. Phys.*, vol. 17, no. 10, 1969, pp. 683–725.

Table 1. Abrasion Cross Sections for Neutron ^{12}C

A_f	Abrasion cross section, mb, for—	
	First-order model	Second-order model
$T = 100$ MeV		
11	139.0	151.3
10	69.9	63.6
9	35.4	22.5
8	15.1	6.1
7	5.1	1.2
6	1.4	0.2
5	0.3	<0.1
$T = 200$ MeV		
11	132.4	132.6
10	52.3	53.4
9	18.8	19.6
8	5.4	5.7
7	1.2	1.3
6	0.2	0.2
$T = 300$ MeV		
11	128.6	127.3
10	46.7	51.8
9	15.1	19.8
8	3.9	6.1
7	0.8	1.5
6	0.1	0.3

Table 2. Abrasion Cross Sections for Neutron ^{27}Al

A_f	Abrasion cross section, mb, for—	
	First-order model	Second-order model
$T = 100$ MeV		
26	192.6	231.9
25	112.5	125.0
24	77.8	61.4
23	50.6	24.4
22	28.9	7.8
21	14.2	2.0
20	6.0	0.4
19	2.2	<0.1
$T = 200$ MeV		
26	201.0	202.1
25	105.1	106.6
24	56.6	56.9
23	26.3	25.9
22	10.3	9.8
21	3.4	3.1
20	0.9	0.8
19	0.2	0.2
$T = 300$ MeV		
26	201.2	189.7
25	99.6	100.8
24	49.0	57.9
23	20.5	29.5
22	7.2	12.8
21	2.1	4.7
20	0.5	1.5
19	0.1	0.4

Table 3. Abrasion Cross Sections for Neutron ^{64}Cu

A_f	Abrasion cross section, mb, for—	
	First-order model	Second-order model
$T = 100$ MeV		
63	255.4	310.9
62	155.0	212.1
61	125.0	153.3
60	106.7	97.2
59	87.2	52.4
58	65.4	24.2
57	44.2	9.6
56	26.8	3.4
$T = 200$ MeV		
63	282.8	286.0
62	177.8	183.2
61	129.4	132.5
60	87.8	87.2
59	52.6	49.9
58	27.5	24.6
57	12.6	10.6
56	5.1	4.0
$T = 300$ MeV		
63	291.5	267.4
62	190.2	165.0
61	122.9	123.5
60	76.0	88.9
59	40.8	57.4
58	19.0	32.7
57	7.7	16.4
56	2.7	7.3

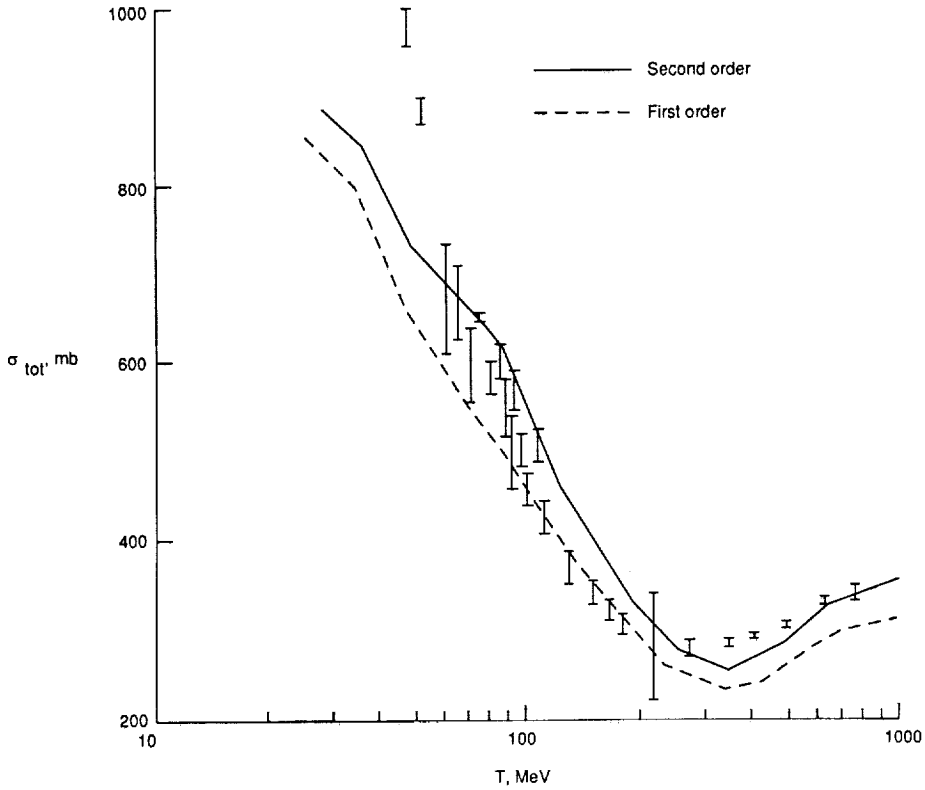

Figure 1. Total cross section for neutron ^{12}C scattering versus neutron energy. Error bars are experimental values.

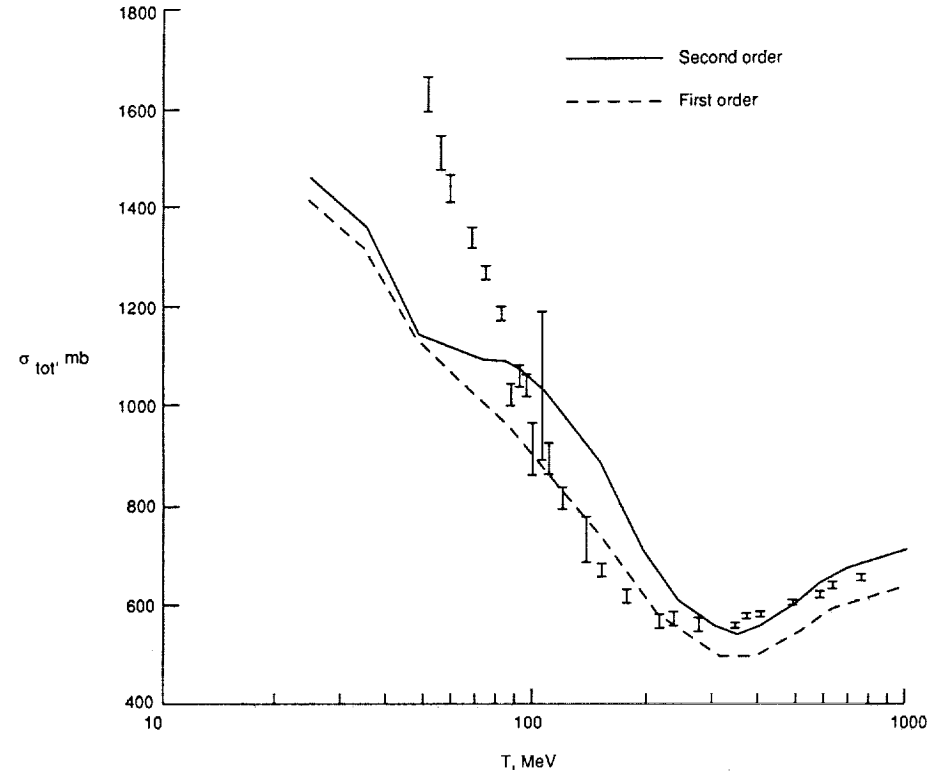

Figure 2. Total cross section for neutron ^{27}Al scattering versus neutron energy. Error bars are experimental values.

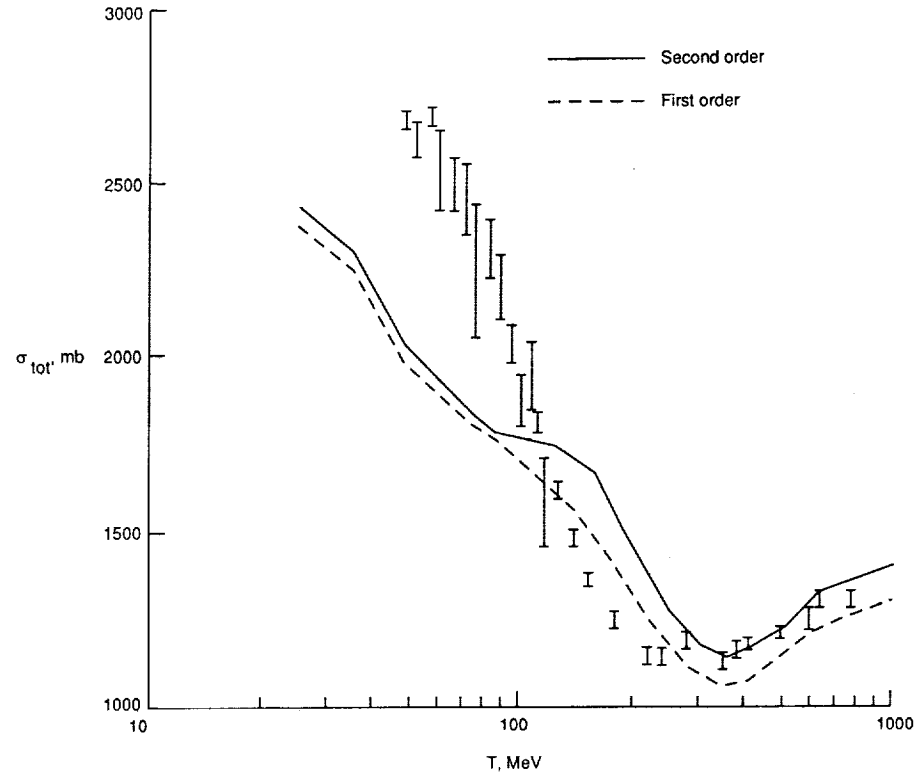

Figure 3. Total cross section for neutron ^{64}Cu scattering versus neutron energy. Error bars are experimental values.

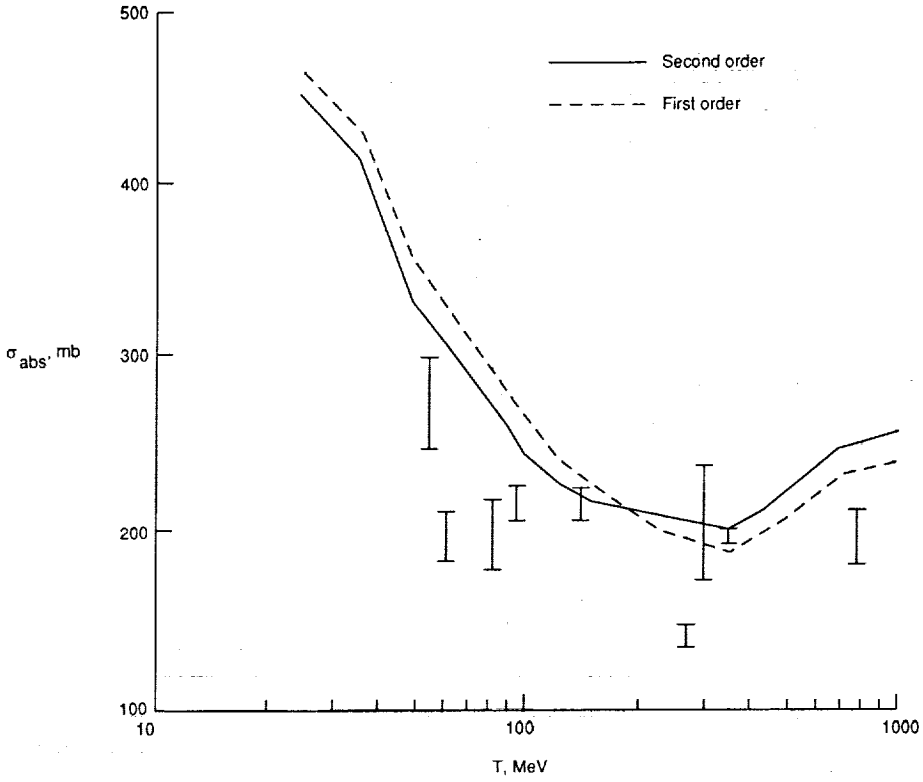

Figure 4. Absorption cross section for neutron ^{12}C scattering versus neutron energy. Error bars are experimental values.

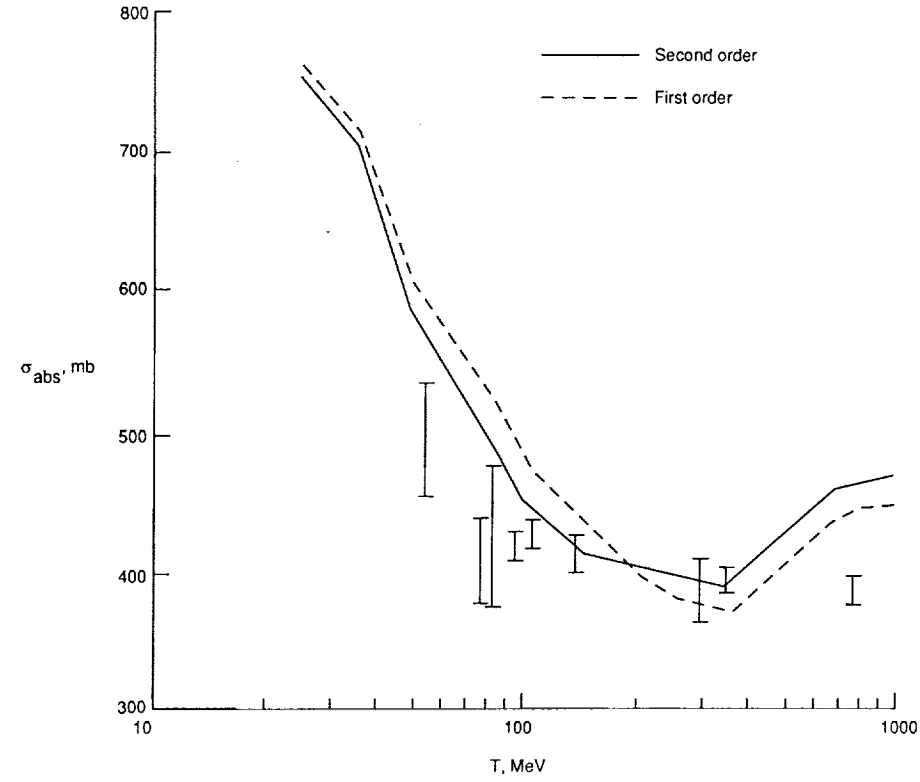

Figure 5. Absorption cross section for neutron ^{27}Al scattering versus neutron energy. Error bars are experimental values.

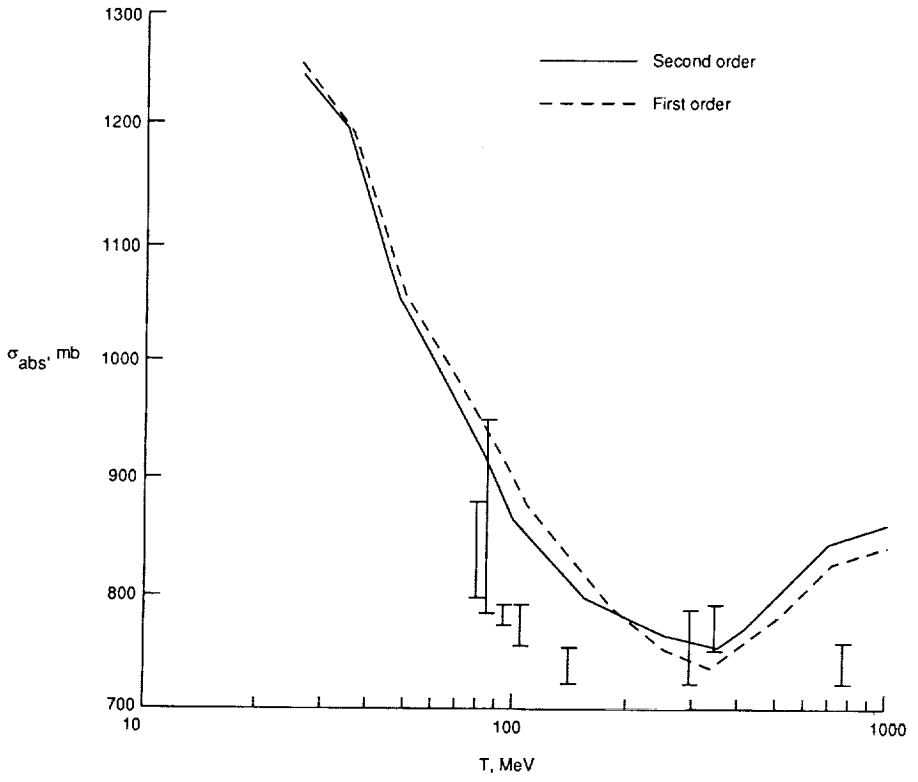

Figure 6. Absorption cross section for neutron ^{64}Cu scattering versus neutron energy. Error bars are experimental values.

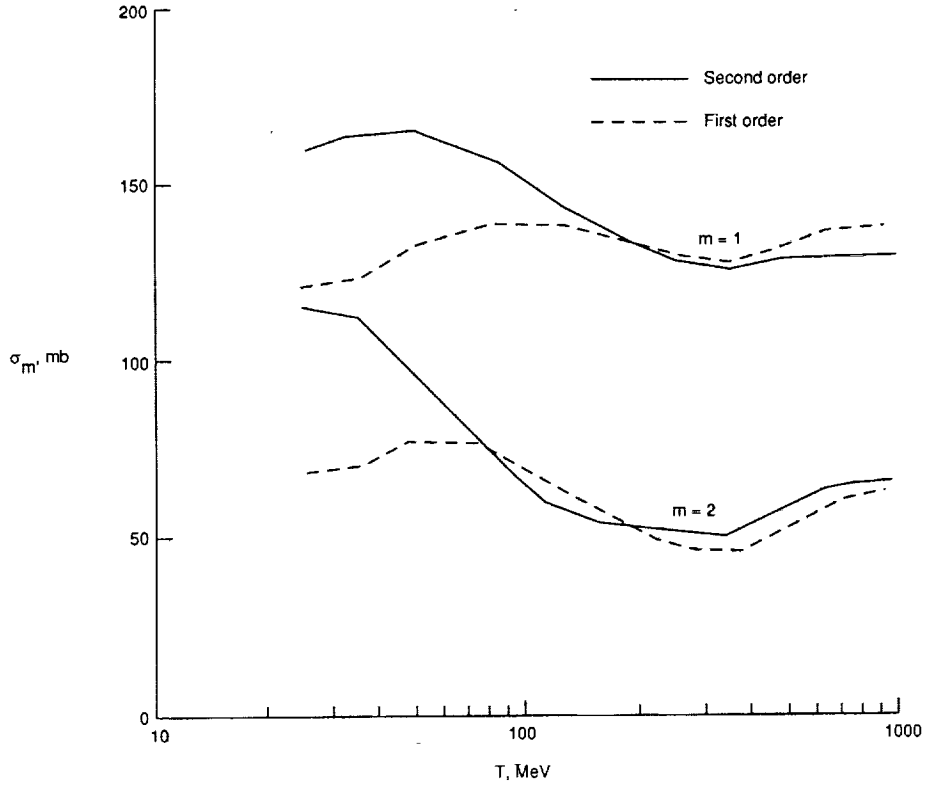

(a) One- and two-nucleon removal.

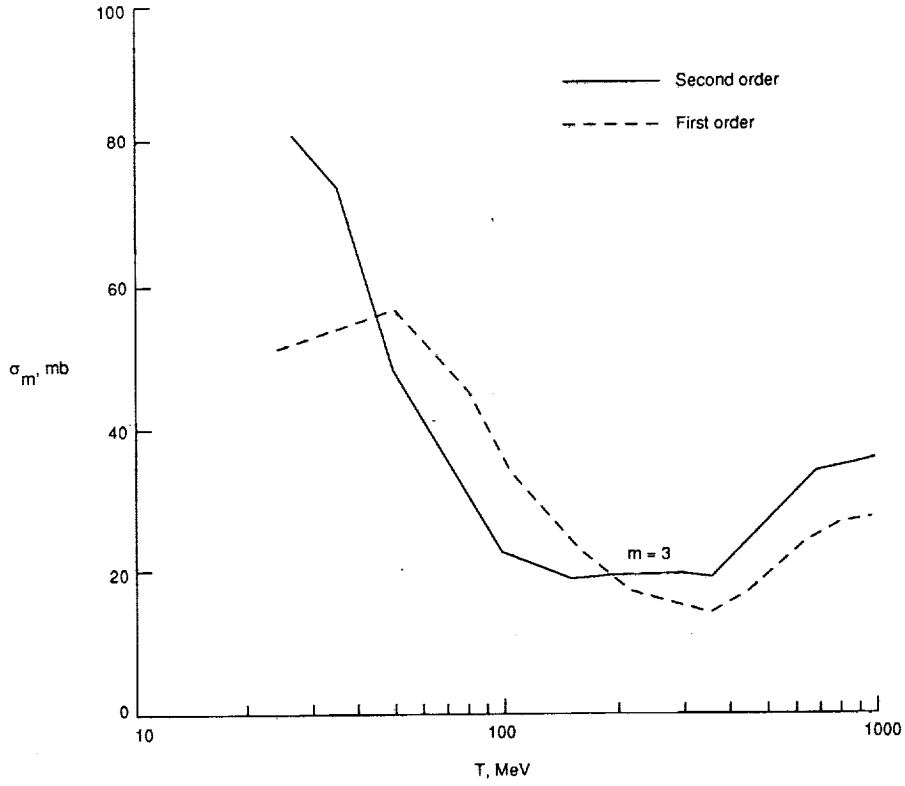

(b) Three-nucleon removal.

Figure 7. Abrasion cross section for neutron ^{12}C scattering versus neutron energy.

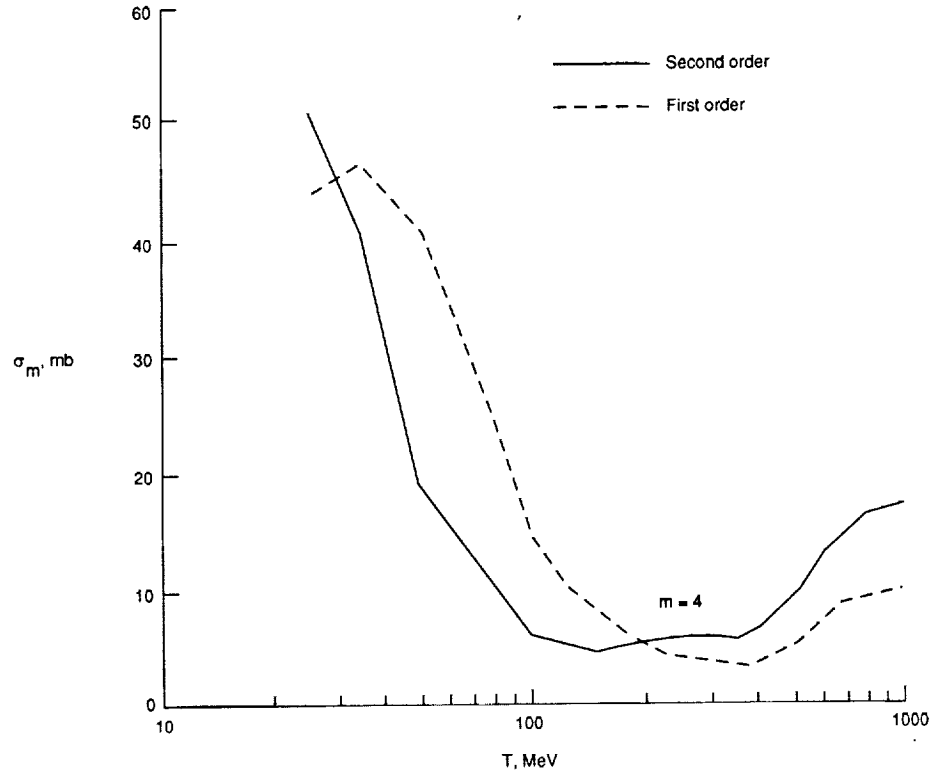

(c) Four-nucleon removal.

Figure 7. Concluded.

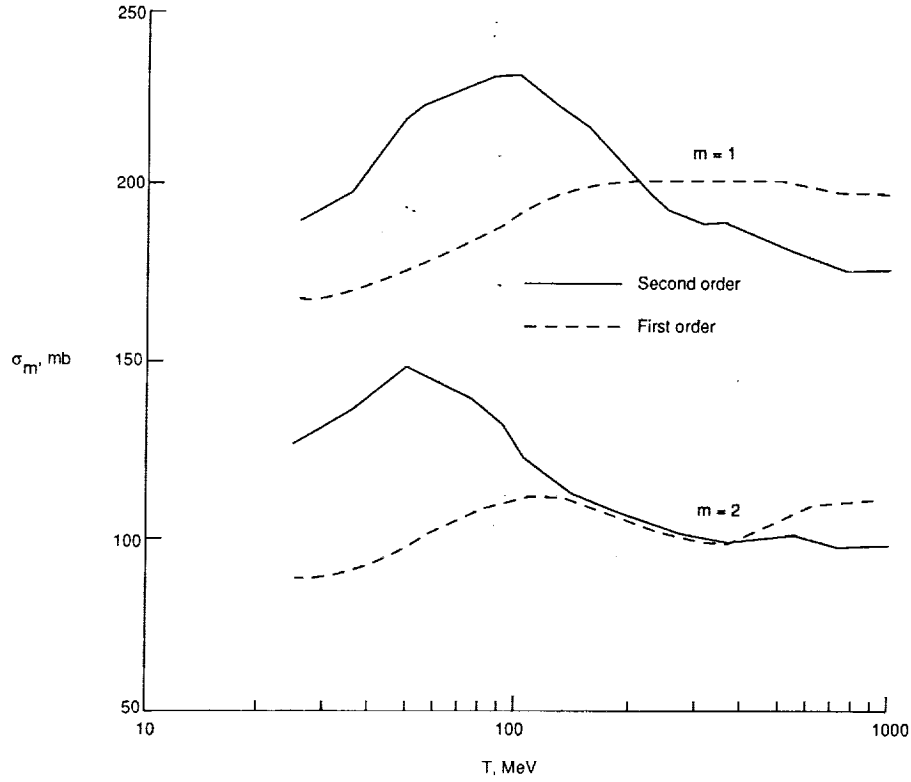

(a) One- and two-nucleon removal.

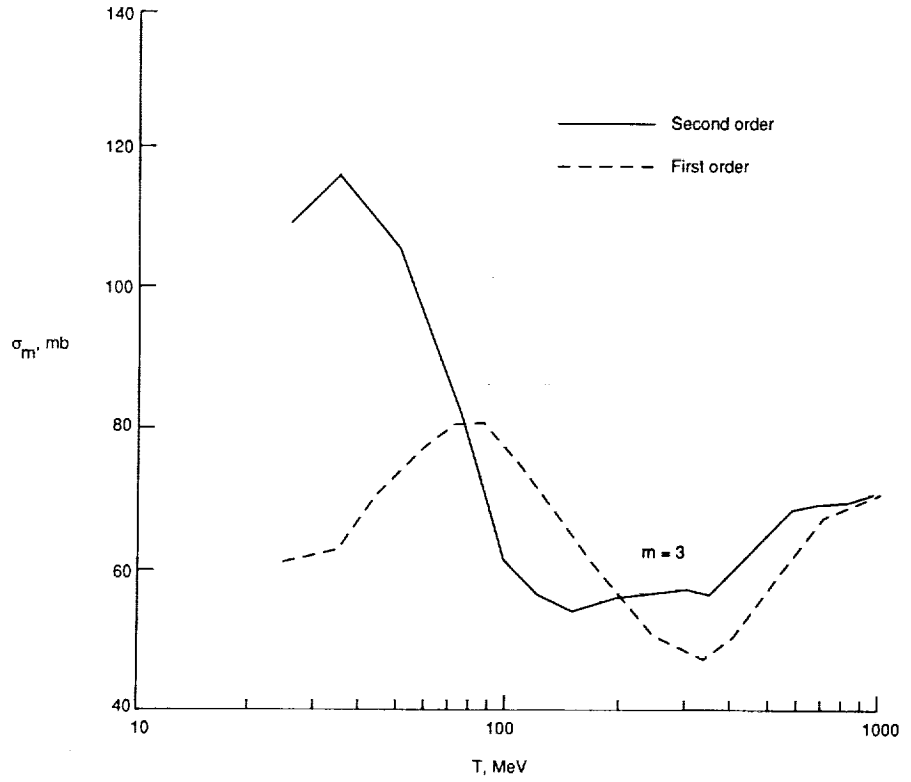

(b) Three-nucleon removal.

Figure 8. Abrasion cross section for neutron ^{27}Al scattering versus neutron energy.

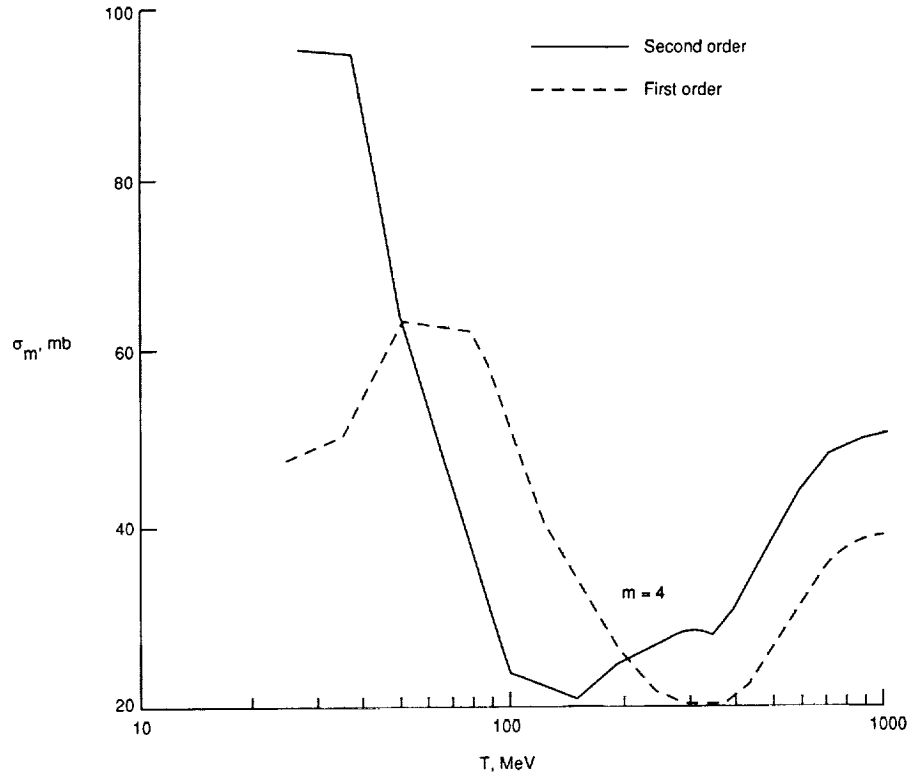

(c) Four-nucleon removal.

Figure 8. Concluded.

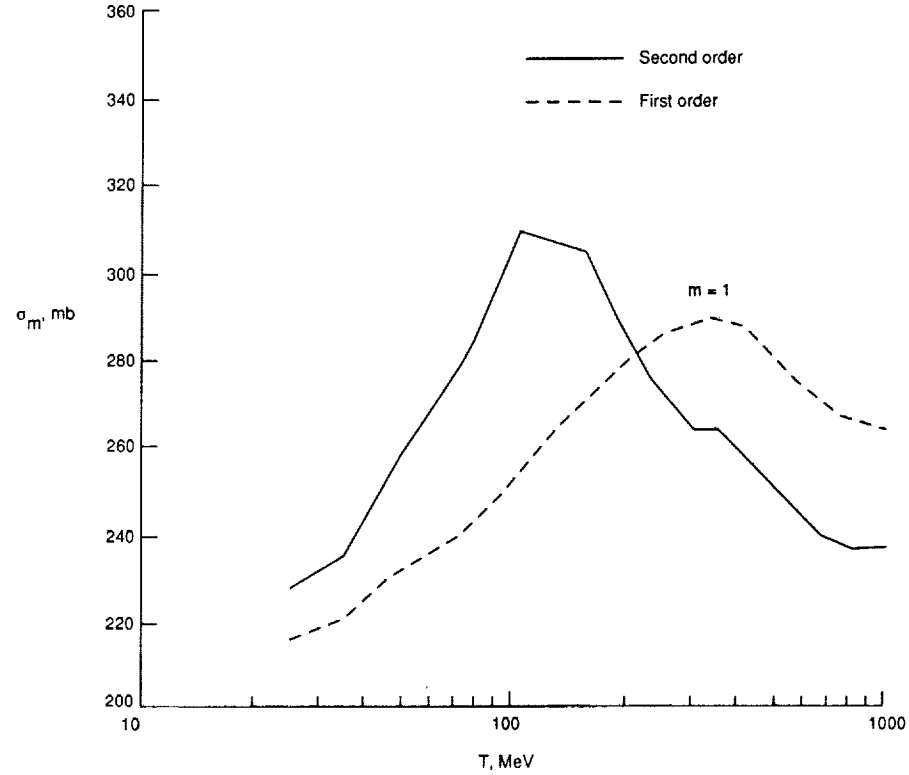

(a) One-nucleon removal.

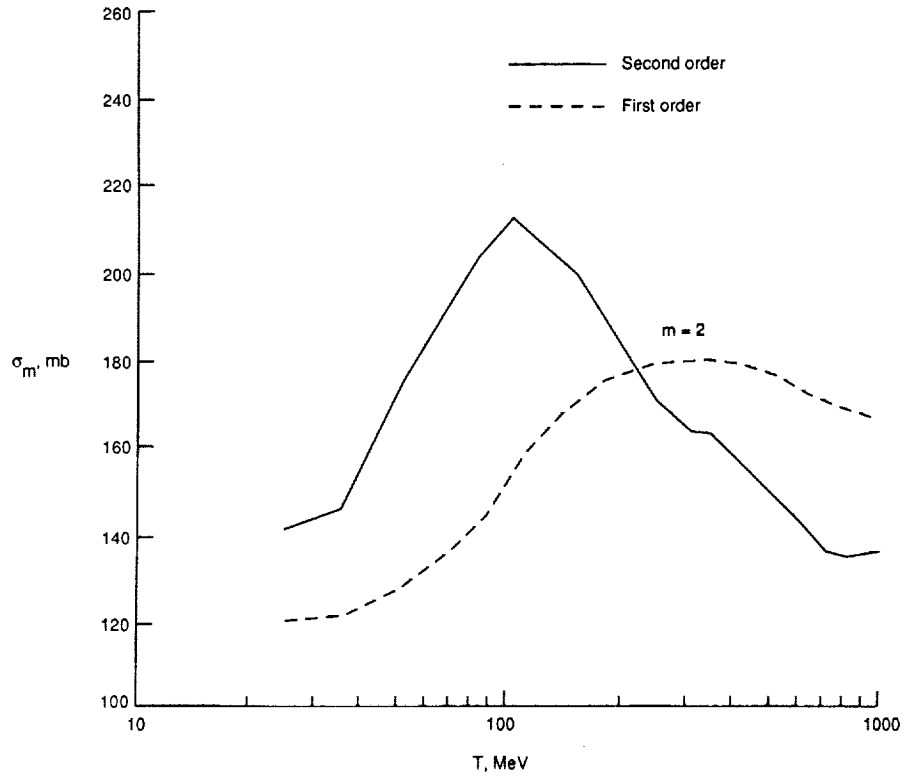

(b) Two-nucleon removal.

Figure 9. Abrasion cross section for neutron ^{64}Cu scattering versus neutron energy.

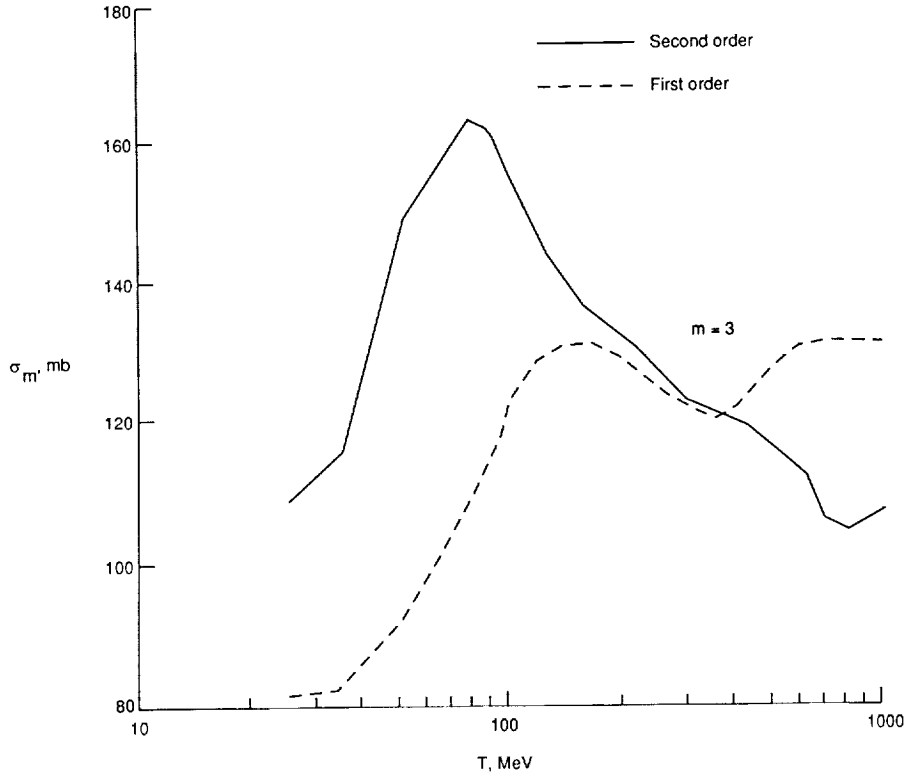

(c) Three-nucleon removal.

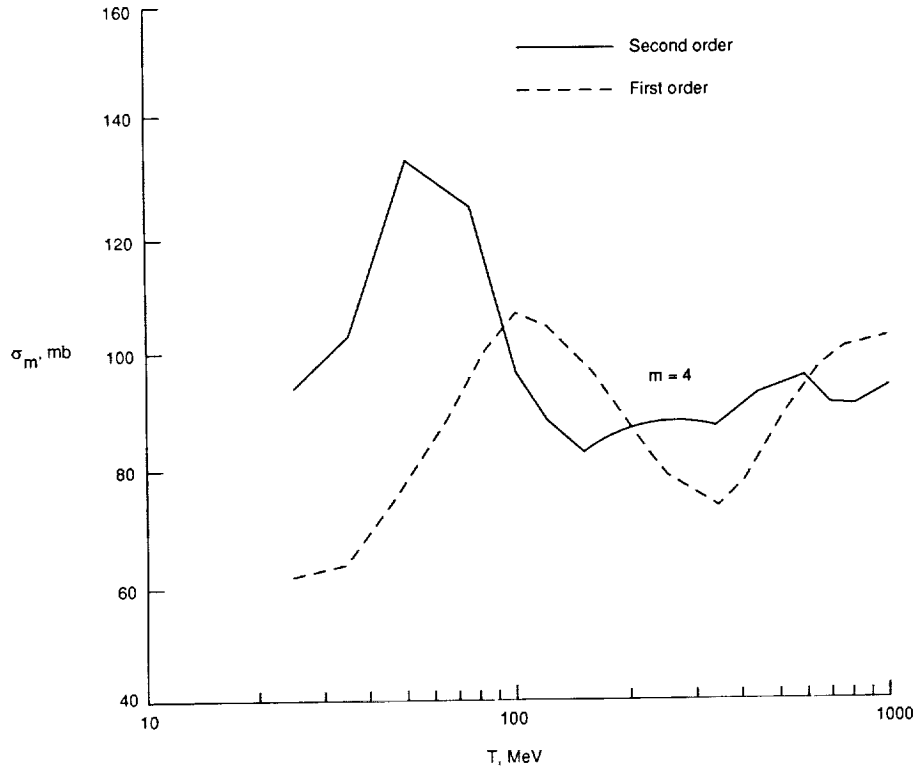

(d) Four-nucleon removal.

Figure 9. Concluded.

REPORT DOCUMENTATION PAGE

Form Approved
OMB No. 0704-0188

1. AGENCY USE ONLY *(Leave blank)*	2. REPORT DATE	3. REPORT TYPE AND DATES COVERED
	December 1991	Technical Memorandum

4. TITLE AND SUBTITLE
Target Correlation Effects on Neutron-Nucleus Total, Absorption, and Abrasion Cross Sections

5. FUNDING NUMBERS
WU 199-04-16-11

6. AUTHOR(S)
Francis A. Cucinotta, Lawrence W. Townsend, and John W. Wilson

7. PERFORMING ORGANIZATION NAME(S) AND ADDRESS(ES)
NASA Langley Research Center
Hampton, VA 23665-5225

8. PERFORMING ORGANIZATION REPORT NUMBER
L-16955

9. SPONSORING/MONITORING AGENCY NAME(S) AND ADDRESS(ES)
National Aeronautics and Space Administration
Washington, DC 20546-0001

10. SPONSORING/MONITORING AGENCY REPORT NUMBER
NASA TM-4314

11. SUPPLEMENTARY NOTES

12a. DISTRIBUTION/AVAILABILITY STATEMENT
Unclassified Unlimited

Subject Category 73

12b. DISTRIBUTION CODE

13. ABSTRACT *(Maximum 200 words)*

Second-order optical model solutions to the elastic scattering amplitude were used to evaluate total, absorption, and abrasion cross sections for neutron-nucleus scattering. Improved agreement with experimental data for total and absorption cross sections is found when compared with first-order (coherent approximation) solutions, especially below several hundred MeV. At higher energies, the first- and second-order solutions are similar. There are also large differences in abrasion cross-section calculations; these differences indicate a crucial role for cluster knockout in the abrasion step.

14. SUBJECT TERMS	15. NUMBER OF PAGES
Heavy ions; Fragmentation; Correlation effects	18
	16. PRICE CODE A03

17. SECURITY CLASSIFICATION OF REPORT	18. SECURITY CLASSIFICATION OF THIS PAGE	19. SECURITY CLASSIFICATION OF ABSTRACT	20. LIMITATION OF ABSTRACT
Unclassified	Unclassified		

NSN 7540-01-280-5500

Standard Form 298(Rev. 2-89)
Prescribed by ANSI Std. Z39-18
298-102

NASA-Langley, 1991